DOI: 10.1002/ejoc.200900601

First Synthesis of *meso*-Chlorinated Tetrabenzoporphyrins

Satoshi Ito,*[a] Le Thanh Phong,[a] Takuya Komatsu,[a] Nagisa Igarashi,[a] Saika Otsubo,[b] Yoshimasa Sakai,[b] Akira Ohno,[b] Shinji Aramaki,[b] Yousuke Tanaka,[c][‡] Hidemitsu Uno,*[c][‡] Toru Oba,[a] and Kazuhisa Hiratani[a]

Keywords: Porphyrinoids / Halogenation / Aromatic substitution / Dyes/Pigments / Cleavage reactions

meso-Chlorinated bicyclo[2.2.2]octadiene-fused porphyrins **2** (Cl_nTBCODPs; n = 1–4) have been synthesized by chlorination of the free base TBCODP-H_2 (**1**-H_2) using *N*-chlorosuccinimide (NCS). The chlorinated derivatives were easily separated by column chromatography on silica gel to give **2**-H_2 in good yields. This method for the chlorination of porphyrin using NCS is mild, safe, and economic compared with the established procedure for the *meso*-chlorination of porphyrins. We also discovered the unexpected *meso*-chlorination of the porphyrin with dichlorodicyanobenzoquinone (DDQ) by single-electron transfer. Cl_nTBCODPs **2** were converted into tetrabenzoporphyrins (Cl_nTBPs) **3** in 100 % yields by retro-Diels–Alder reaction. The derived compounds were characterized by NMR spectroscopy, UV/Vis spectrophotometry, cyclic voltammetry (CV), X-ray crystallography, and organic field-effect transistor (OFET) characteristics. The introduction of chlorine at the *meso* positions of the TBPs drastically changed their electronic and structural properties. The maxima of protonated Cl_4TBP-H_2 (**3d**-H_2; λ_{max} = 494, 649, and 707 nm) were redshifted by around 50–65 nm relative to those of protonated TBP-H_2 (λ_{max} = 431, 605, and 660 nm). The two Q-band maxima of the Cl_4TBP dication are similar to those of a tetraacenaphthoporphyrin dication (λ_{max} = 525, 646, and 702 nm), which has one of the most redshifted Q-bands.

Introduction

Tetrabenzoporphyrin (TBP) has a similar skeletal alignment as phthalocyanine, which is one of the most common and useful dyes. TBP was first prepared from carboxymethylphthalide under harsh conditions (345–420 °C) by Linstead and Noble in 1937.[1] Recently, TBP and phthalocyanine derivatives have attracted considerable attention as organic semi-conducting materials for field-effect transistors (OFET),[2] near-IR dyes,[3] nonlinear optical materials,[4] and as photosensitizers for photodynamic therapy (PDT) of cancer tissues.[5] Fine-tuning of the chemical and physical properties of these dye stuffs is very important for their application. From this point of view, TBP derivatives are thought to be more advantageous than phthalocyanines because the electronic and structural properties of the porphyrin derivatives can be effectively modified by the introduction of substituents at the *meso* positions.[6] The electronic effects of substituents are generally larger at the *meso* positions than at the β positions due to a quite different contribution of atomic orbitals of the *meso* atoms to the HOMO and HOMO–1 of porphyrin.[7] The introduction of *meso* substituents is only possible for TBP, although direct *meso* substitutions of β-octasubstituted porphyrins, including TBP, have been limited due to steric hindrance of the β-functional groups.[8] Moreover, TBP and their derivatives are insoluble in almost all common solvents. Therefore, few examples of the preparation of substituted TBPs, with the exception of simple aryl groups, have been reported.[9] The introduction of halogen atoms at the *meso* positions of TBPs is thought to be very important, not only because of the modification of their electronic states and structural properties, but also because of their possible conversion into various functionalized TBPs by nucleophilic and coupling reactions.[10] We have previously reported the simple and clean synthesis of TBPs from quadruply bicyclo[2.2.2]-octadiene-fused porphyrins (TBCODPs) as soluble precursors of TBPs by a retro-Diels–Alder reaction[11] and applied TBPs for fabrication of OFETs based on the solution process.[12] In this paper, we report the first synthesis, proper-

[a] Department of Applied Chemistry, Faculty of Engineering, Utsunomiya University,
7-1-2 Yotou, Utsunomiya, Tochigi 321-8585, Japan
Fax: +81-28-689-7013
E-mail: s-ito@cc.utsunomiya-u.ac.jp
[b] Mitsubishi Chemical Group, Science and Technology Research Center, Inc.,
1000 Kamoshida-cho, Aoba-ku, Yokohama 227-8502, Japan
[c] Division of Synthesis and Analysis, Department of Molecular Science, Integrated Center for Science, Ehime University, Matsuyama 790-8585, Japan
[‡] Present address: Department of Chemistry and Biology, Graduate School of Science and Engineering, Ehime University, Matsuyama 790-8577, Japan
Fax: +81-89-927-9610
E-mail: uno@dpc.ehime-u.ac.jp
Supporting information for this article is available on the WWW under http://dx.doi.org/10.1002/ejoc.200900601.

ties, and crystal structures of *meso*-chlorinated tetrabenzoporphyrins (Cl_nTBPs) **3** by chlorination of the free base TBCODP-H_2 (**1**-H_2) using *N*-chlorosuccinimide (NCS) or DDQ followed by a retro-Diels–Alder reaction.

Results and Discussion

Preparation of Chlorinated TBCODPs and TBPs

After the initial research by Nencki and Zaleski,[13] the chlorination of porphyrins was systematically studied by Fischer and co-workers, although their structural assignments were problematic due to the absence of reliable analytical methods.[14] The chlorination of all β-substituted porphyrins required harsh reaction conditions. Bonnett et al. reported that the reaction of octaethylporphyrin (OEP) with concentrated HCl and H_2O_2 in 0.5 M hydrochloric acid gave various *meso*-chlorooctaethylporphyrins (Cl_nOEPs).[15] Gong and Dolphin reported the conversion of the *meso*-tetranitrooctaethylporphyrin–zinc complex into Cl_4OEP–Zn by treatment with hydrochloric acid.[16] However, these established chlorination methods could not be applied to the preparation of chlorinated TBCODPs because the bicyclo[2.2.2]octadiene functional groups are reactive under harsh electrophilic conditions. On the other hand, sterically unhindered porphyrins such as 5,15-diaryl- and 5,10,15-triarylporphyrins readily undergo chlorination at the unsubstituted *meso* positions on treatment with $PhICl_2$.[17]

During our investigation of the thermal behavior of TBCODP-H_2 (**1**-H_2) under various conditions, we detected the unexpected formation of Cl_nTBPs **3** by MALDI-TOF mass spectral analysis of the thermal decomposition of **1**-H_2 in *o*-dichlorobenzene at 120 °C in the presence of a large excess of DDQ. The chlorination of TBCODP-H_2 (**1**-H_2) was expected to occur prior to the retro-Diels–Alder reaction [Equation (1)] because TBP is poorly soluble even in hot *o*-dichlorobenzene. We carried out the reaction of **1**-H_2 with 15 equiv. of DDQ in *o*-dichlorobenzene at a lower temperature (80 °C) for 48 h. The tetrachloro derivative (Cl_4TBCODP-H_2, **2d**-H_2) was isolated as Cl_4TBCODP–Zn (**2d**-Zn) in 28% yield by chromatographic purification after metallation with zinc acetate. When TBCODP–Zn (**1**-Zn) was employed instead of **1**-H_2, a complex mixture was obtained probably due to demetalation with hydrogen chloride generated by the decomposition of DDQ.[18] In fact, the reaction mixture was strongly acidic at the end of reaction.

To identify the chlorination mechanism, UV/Vis spectra[11] of **1**-H_2 were recorded in the presence and absence of 10 equiv. of DDQ (Figure 1). Quite a large redshift (24 nm) of the Soret-band absorption was observed in the presence of DDQ (410 nm). There were four obvious Q-band absorptions between 470 and 650 nm in the absence of DDQ, and large unresolved Q-band absorptions were observed at over 530 nm in the presence of DDQ. These facts clearly indicate the formation of a complex between **1**-H_2 and DDQ. A possible reaction mechanism for this chlorination reaction is illustrated in Scheme 1.

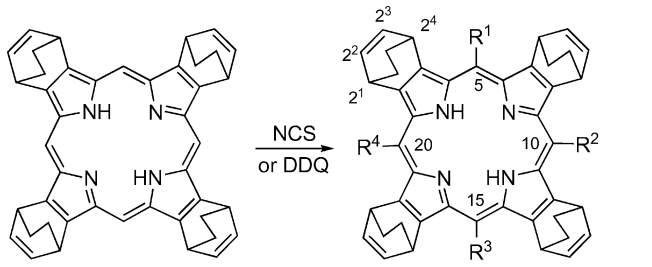

1-H_2

2a-H_2: R^1 = Cl; R^2 = R^3 = R^4 = H
adj-**2b**-H_2: R^1 = R^2 = Cl; R^3 = R^4 = H
opp-**2b**-H_2: R^1 = R^3 = Cl; R^2 = R^4 = H
2c-H_2: R^1 = R^2 = R^3 = Cl; R^4 = H
2d-H_2: R^1 = R^2 = R^3 = R^4 = Cl

(1)

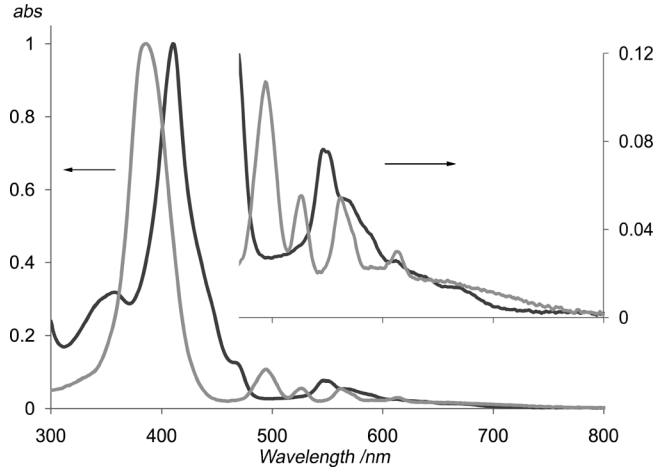

Figure 1. UV/Vis spectra of **1**-H_2 in the presence (black line) and absence (grey line) of 10 equivs. of DDQ.

Single-electron transfer from TBCODP-H_2 (**1**-H_2) to DDQ could occur to afford porphyrin cation radical **1**-$H_2^{\cdot+}$, which should be more stable than usual β-octaalkylporphyrin cation radicals such as $OEP^{\cdot+}$ because **1**-$H_2^{\cdot+}$ has no hyperconjugative hydrogen atom. A chloride ion generated by the decomposition of DDQ in solvent then attacks the *meso* carbon atom of **1**-$H_2^{\cdot+}$ to form a chlorinated porphyrin radical which would give ClTBCODP-H_2 (**2a**-H_2) on further oxidation with DDQ followed by loss of a proton. This chlorination cycle would then be repeated to give Cl_4TBCODP-H_2 (**2d**-H_2).

Because we failed to improve the chlorination of **1** with DDQ in spite of our efforts, other chlorination methods were examined, and *N*-chlorosuccinimide (NCS) was found to be suitable for use as the chlorinating reagent. TBCODP-H_2 (**1**-H_2) reacted with 1.1–4.4 equiv. of NCS in chloroform under argon at 75 °C for 12–72 h. Fortunately, chlorinated derivatives were easily separated by column chromatography on silica gel (hexane/chloroform, 4:1; R_f values for **2a**-H_2, *adj*-**2b**-H_2, *opp*-**2b**-H_2, **2c**-H_2, and **2d**-H_2 were approx. 0.30, 0.40, 0.55, 0.75, and 0.80, respectively) to give

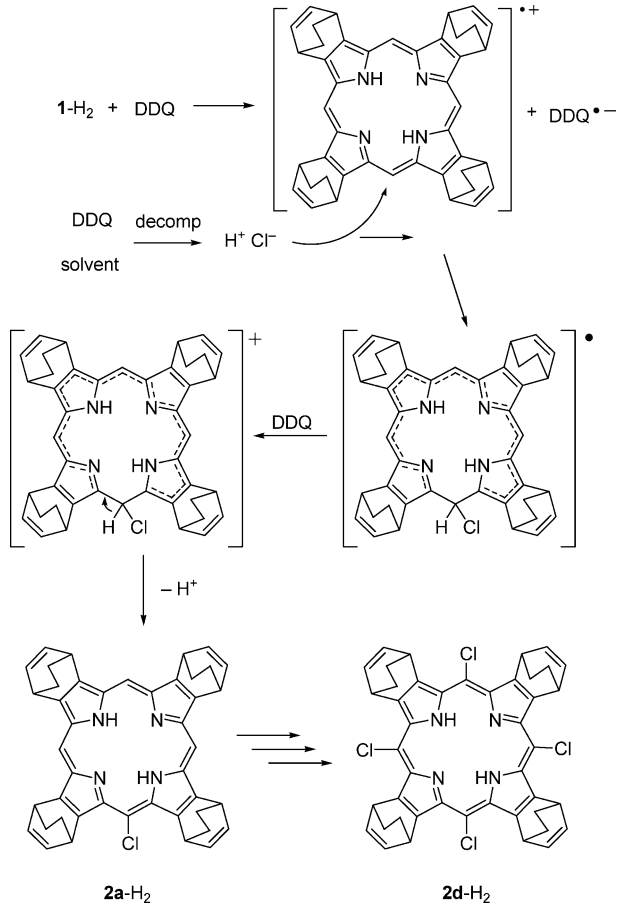

Scheme 1. Possible reaction mechanism for the chlorination of **1**-H_2 with DDQ.

2-H_2 in acceptable combined yields of 55–70% (Table 1), and no thermally decomposed products were detected. In general, multiple chlorination of an aromatic ring with electrophilic reagents is difficult because the introduced chlorine atom deactivates the aromatic ring. However, oligochlorination of **1**-H_2 easily proceeded even with only 1.1 equiv. of NCS (Entry 1). In this case, the dichloro (*adj*-**2b**-H_2 and *opp*-**2b**-H_2; 11% combined yield) and trichloro derivatives (**2c**-H_2; trace) were obtained in addition to ClTBCODP-H_2 (**2a**-H_2; 43% yield). Although we failed to find the conditions for the preferential formation of the di- and trichloro derivatives, the reaction with 4.4 equiv. of NCS afforded tetrachloroporphyrin **2d**-H_2 in a fair yield (70%, Entry 4) in addition to the trichloroporphyrin **2c**-H_2 (13%). In all cases *opp*-**2b**-H_2 was slightly favored over *adj*-**2b**-H_2. The zinc complexes Cl_nTBCODP–Zn (**2**-Zn) were readily prepared in quantitative yields by the conventional method, and Cl_nTBCODP–M (M = H_2 and Zn) were converted into pure Cl_nTBP–M (**3a**-M, *adj*-**3b**-M, *opp*-**3b**-M, **3c**-M, and **3d**-M) in quantitative yields at 200 °C in vacuo in 10 min [Equation (2)].

When similar conditions were applied to the chlorination of the free-base OEP by using 4.4 equiv. of NCS, chlorination preferentially occurred at the ethyl groups. Only the

Table 1. Chlorination of **1**-H_2 with NCS in chloroform at reflux.

Entry	Equiv. of NCS	Yield [%][a]				
		2a-H_2	*adj*-**2b**-H_2	*opp*-**2b**-H_2	**2c**-H_2	**2d**-H_2
1	1.1	43	3	8	trace	0
2	2.2	18	32	33	5	trace
3	3.3	4	13	24	28	9
4	4.4	0	trace	trace	13	70

[a] Isolated yield, by column chromatography.

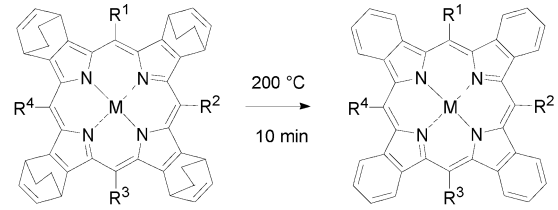

M = H_2 or Zn
2a-M: R^1 = Cl; R^2 = R^3 = R^4 = H
adj-**2b**-M: R^1 = R^2 =Cl; R^3 = R^4 = H
opp-**2b**-M: R^1 = R^3 =Cl; R^2 = R^4 = H
2c-M: R^1 = R^2 = R^3 = Cl; R^4 = H
2d-M: R^1 = R^2 = R^3 = R^4 = Cl

M = H_2 or Zn
3a-M: R^1 = Cl; R^2 = R^3 = R^4 = H
adj-**3b**-M: R^1 = R^2 =Cl; R^3 = R^4 = H
opp-**3b**-M: R^1 = R^3 =Cl; R^2 = R^4 = H
3c-M: R^1 = R^2 = R^3 = Cl; R^4 = H
3d-M: R^1 = R^2 = R^3 = R^4 = Cl (2)

5-chloro (**4a**-H_2) and 5,15-dichloro derivatives (*opp*-**4b**-H_2) were isolated in small amounts (33 and 16%, respectively) in addition to an intractable mixture of compounds multichlorinated at the *meso* positions and on the ethyl substituents [Equation (3)].[19]

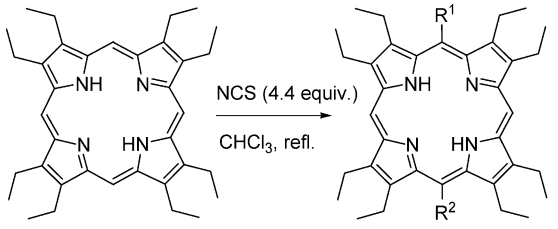

4a-H_2: R^1 = Cl; R^2 = H
opp-**4b**-H_2: R^1 = R^2 =Cl (3)

Electronic and Structural Properties of the Cl_nTBCODPs

In general, the absorption spectra of porphyrins are known to be greatly affected not only by the electronic properties of substituents but also by the deformation of the porphyrin rings.[6] Although the substituents of TBCODP and OEP consist of only hydrocarbons, the electronic properties are quite different because TBCODPs have no hyperconjugative hydrogen atom. Therefore, the energy gaps between two degenerate LUMOs and two of the highest MOs in TBCODPs are larger than those in OEPs. In fact, the Soret band absorption of TBCODP-H_2 (**1**-H_2) was 11 nm lower than that of OEP-H_2.[11] The introduction of chlorine atoms at the *meso* positions should distort the

porphyrin rings by steric repulsion with the β-substituents, which leads to a redshift of the UV absorption bands, a decrease of the macrocyclic ring current, and an increase of the reactivity towards electrophilic reagents.[6] The absorption spectra of Cl_nTBCODP-H_2 (**2**-H_2) are shown in Figure 1. The absorption maxima of Cl_nTBCODP-H_2 are redshifted by around 10 nm per chlorine atom introduced. These values are blueshifted by about 10 nm relative to those of the corresponding Cl_nOEP.[15,16] In the ^{1}H NMR spectra, the NH absorption signal of ClTBCODP-H_2 (**2a**-H_2; δ = –4.10 ppm) appears 0.70 ppm lower than that of TBCODP-H_2 (**1**-H_2; δ = –4.80 ppm), whereas that of ClOEP-H_2 (**4a**-H_2; δ = –3.13 ppm) appears 0.60 ppm lower than that of OEP-H_2 (δ = –3.74 ppm). These results clearly suggest that the Cl_nTBCODPs are more planar than the corresponding Cl_nOEPs in solution. The ^{1}H NMR spectra of Cl_nTBCODP-H_2 (**2**-H_2) are shown in Figure 2 and clearly indicate that the anisotropic effect of the porphyrin ring becomes weaker with increasing numbers of introduced chlorine atoms. Although the β-fused BCOD group is considered to be smaller than β,β′-diethyl groups, the accumulation of *meso*-chlorine substituents would bring about a severe deformation of the porphyrin ring in TBCODP.

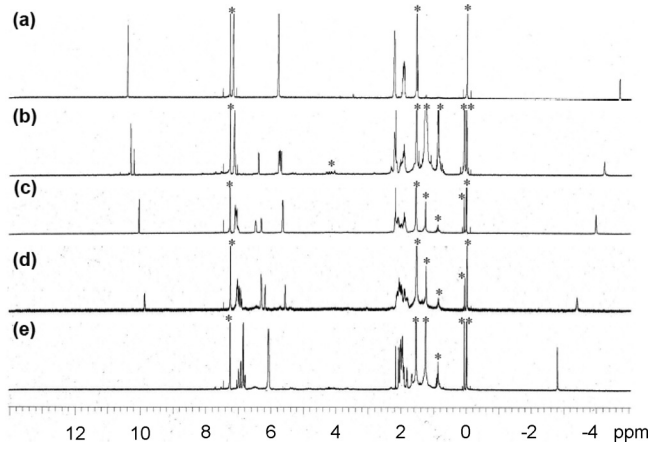

Figure 2. NMR spectra of (a) **1**-H_2, (b) **2a**-H_2, (c) *adj*-**2b**-H_2, (d) **2c**-H_2, and (e) **2d**-H_2 in $CDCl_3$. Signals with an asterisk denote solvent peaks.

Next, we tried to obtain single crystals of the chlorinated porphyrins to determine their structures. The chlorinated porphyrins (Cl_nTBCODPs and Cl_nOEPs) were dissolved in chloroform or pyridine, and then the solutions were placed in methanol vapor. All the Cl_nTBCODPs used were diastereomeric mixtures based on the BCOD orientation. Single crystals of only four Cl_nTBCODPs (**2a**-H_2·$CHCl_3$, *opp*-**2b**-H_2·$CHCl_3$, *opp*-**2b**-Zn·C_5H_5N, and **2d**-Zn·2MeOH) were obtained (see S1 of the Supporting Information). The crystals of *opp*-**2b**-H_2·$CHCl_3$ were apparently clear and rhombohedral. However, twin crystals were obtained, probably because one angle of the cell is nearly perpendicular. Twin treatment of the data did not improve the result.

In each crystal of **2a**-H_2·$CHCl_3$ and *opp*-**2b**-H_2·$CHCl_3$, independent porphyrin molecules occupy the special inversion positions, whereas the porphyrin molecule *opp*-**2b**-Zn·C_5H_5N is found in a normal position. Two crystallographically different porphyrin molecules occupy normal positions in **2d**-Zn·2MeOH. From the symmetry demand of the inversion center, the porphyrin molecules in **2a**-H_2·$CHCl_3$ and *opp*-**2b**-H_2·$CHCl_3$ have a waved out-of-plane distortion (Figure 3). Similarly, a waved out-of-plane distortion is observed in *opp*-**2b**-Zn·C_5H_5N. On the other hand, the two independent porphyrin molecules in **2d**-Zn·2MeOH showed a 1,3-alternate out-of-plane distortion, which is commonly found in dodecasubstituted porphyrin–zinc complexes.[20] Although the crystal structural data of *meso*-chlorinated TBCODPs and OEPs could not be compared due to the lack of crystal data for *meso*-chlorinated OEPs, interesting information was obtained. To our surprise, the out-of-plane distortion in the *mono*-chlorinated porphyrin (ClTBCODP-H_2; **2a**-H_2, *opp*-Cl_2TBCODP-H_2; *opp*-**2b**-H_2) is very small, and the largest deviations from the mean plane of 24 porphyrin ring atoms are 0.050(3) (N) and 0.042(4) Å (β-C) in **2a**-H_2 and 0.050(4) (N) and 0.076(7) Å (β-C) in *opp*-**2b**-H_2. These values are almost similar to those of TBCODP-H_2 [**1**-H_2; 0.069(3) Å for N and 0.067(3) Å for β-C].[21] In the case of *opp*-**2b**-Zn·C_5H_5N, a slightly larger distortion is observed, probably due to coordination of a large pyridine ligand to the center zinc atom.

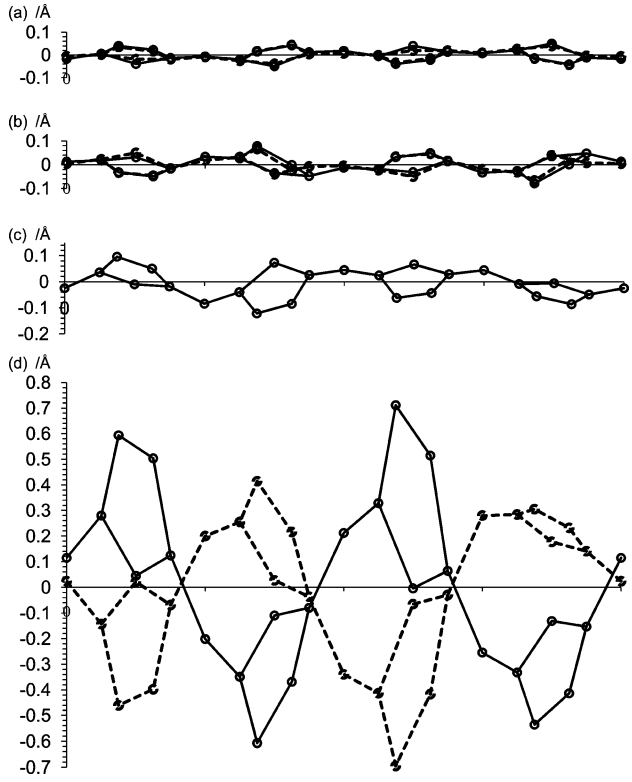

Figure 3. View of the skeletal deviations of the 24 ring atoms from the porphyrin mean plane. (a) **2a**-H_2·$CHCl_3$, two independent molecules; solid and broken lines; (b) *opp*-**2b**-H_2·$CHCl_3$: two independent molecules; solid and broken lines; (c) *opp*-**2b**-Zn·C_5H_5N; (d) **2d**-Zn·2MeOH: two independent molecules; solid and broken lines.

On the other hand, quite a large saddle distortion is observed in **2d**-Zn·2MeOH, and the largest deviation is 0.711(5) Å for the β-C. These facts clearly indicate that the introduction of one chlorine atom does not affect the planarity of the quadruply BCOD-fused porphyrin plane. However, accumulation of chlorine atoms causes severe ring distortion by the buttressing effect. This effect may be one of the reasons for the slightly preferred formation of *opp*-**2b**-H_2 over *adj*-**2b**-H_2.

The oxidation potentials of the Cl_nTBCODP–zinc complexes **2**-Zn were determined by cyclic voltammetry (CV; Table 2). As the number of chlorine atoms increases, the difference between the first and second oxidation potentials becomes smaller, and values of the second oxidation potentials were reduced due to partial irreversibility. Interestingly, the first oxidation potential of *opp*-**2b**-Zn was the highest among those studied. This result is well rationalized by considering the conflicting effects of chlorine introduction: deformation of the porphyrin ring and electron-withdrawing effects. The deformation of the porphyrin ring raises the energy levels of the occupied molecular orbitals, whereas the electron-withdrawing chlorine atom lowers the energy levels. In **2d**-Zn, the porphyrin deformation effect caused by the introduction of three chlorine atoms exceeded the electron-withdrawing effect.

Table 2. Oxidation potentials of Cl_nTBCODP–Zn (**2**-Zn) in CH_2Cl_2.

Porphyrin	$E^{ox}_{1/2}$ (1)[a] [V]	$E^{ox}_{1/2}$ (2)[a] [V]	$E^{ox}_{1/2}$ (2) – $E^{ox}_{1/2}$ (1) [V]
1-Zn	+0.437	+0.878	0.441
2a-Zn	+0.478	+0.783	0.305
adj-**2b**-Zn	+0.490	+0.771	0.281
opp-**2b**-Zn	+0.520	+0.759	0.239
2c-Zn	+0.497	+0.723	0.226
2d-Zn	+0.478	+0.660	0.182

[a] *E* [V] vs. Ag/Ag^+ (Fc/Fc^+ = +0.233 V), 0.1 M TBAP in CH_2Cl_2.

Electronic and Structural Properties of the Cl_nTBPs

The absorption spectra of Cl_nTBPs **3** were recorded in 5% TFA/$CHCl_3$ because Cl_nTBPs **3** are insoluble in most common organic solvents (Figure 4). As the number of chlorine atoms at the *meso* positions increased, the Soret and Q bands of the Cl_nTBP dications were also redshifted by the electron-withdrawing effect and the deformation of the porphyrin ring. In particular, the absorption maxima of protonated Cl_4TBP-H_2 (**3d**-H_2; λ_{max} = 494, 649, and 707 nm) were significantly redshifted by around 50–65 nm relative to those of protonated TBP-H_2 (λ_{max} = 431, 605, and 660 nm).[22] The two Q-band maxima of the Cl_4TBP dication are similar to those of a tetraacenaphthoporphyrin dication (λ_{max} = 525, 646, and 702 nm),[23] which has one of the most redshifted Q-bands.

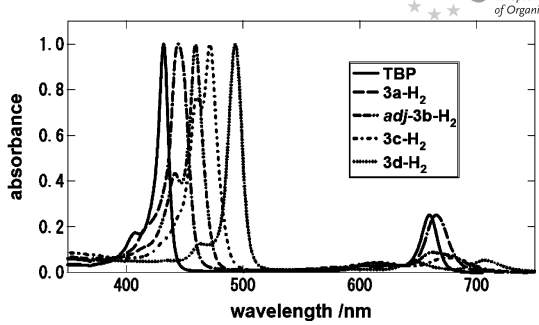

Figure 4. UV/Vis spectra of Cl_nTBPs **3** in 5% TFA/$CHCl_3$.

We attempted to obtain single crystals of the chlorinated TBPs. Although the solubility of chlorinated TBPs is usually poor, Cl_nTBP–zinc complexes (**3**-Zn) are moderately soluble in coordinating solvents such as pyridine and THF. Therefore, the zinc complexes were dissolved in pyridine, and then the solutions were placed in a vapor of methanol or 2-propanol. Single crystals of ClTBP–Zn (**3a**-Zn) and Cl_4TBP–Zn (**3d**-Zn) (**3a**-Zn·3/2C_5H_5N from C_5H_5N/MeOH, **3a**-Zn·3/2C_5H_5N from C_5H_5N/*i*-C_3H_7OH, **3d**-Zn·3/2C_5H_5N·1/2MeOH, and **3d**-Zn·5/4C_5H_5N·3/4*i*-C_3H_7OH) were obtained (see S2 of the Supporting Information).

In the cases of the **3d**-Zn crystals, non-coordinated solvent molecules such as pyridine, 2-propanol, and/or methanol were not properly modeled. Therefore, the structures were refined without these solvents by the PLATON Squeeze technique.[24] Two crystallographically independent porphyrin molecules were found in the crystals of **3a**-Zn·3/2C_5H_5N from C_5H_5N/MeOH, **3a**-Zn·3/2C_5H_5N from C_5H_5N/*i*-C_3H_7OH, and **3d**-Zn·3/2C_5H_5N·1/2MeOH, whereas the **3d**-Zn·5/4C_5H_5N·3/4*i*-C_3H_7OH crystal contained four independent porphyrin molecules. All the porphyrin molecules occupied normal positions. The deviations from the porphyrin mean planes are illustrated in Figure 5. All the monochlorinated TBP molecules show a slightly ruffled out-of-plane distortion (Figure 5a,b), whereas Cl_4TBP–Zn molecules adopt ruffled and saddle out-of-plane conformations depending on the mode of stacking. ORTEP diagrams viewed perpendicular to the axis of stacked pairs of Cl_4TBP–Zn molecules in these crystals are illustrated in Figure 6. Two independent Cl_4TBP–Zn molecules in the crystal of $P\bar{1}$ completely eclipse each other, and two molecules of pyridine are coordinated from the outside of this stacking pair (Figure 6a). An interesting stacking diagram is observed in the case of the **3d**-Zn·5/4C_5H_5N·3/4*i*-C_3H_7OH crystal ($P2_1/c$). The independent molecules **A** and **B** are stacked in such a way that they are completely eclipsed, similarly to the $P\bar{1}$ crystal, and exhibit a large 1,3-alternate out-of-plane distortion (Figure 5d and Figure 6b). On the other hand, one of the benzene rings of molecule **D** is situated above the center zinc atom of molecule **C**, and the rotating angle of these porphyrin molecules is approximately 17.7° (Figure 6c). Moreover, these molecules show intermediate out-of-plane distortion of ruffling and sad-

dling, although the ruffling is slightly greater than the saddling (Figure 5d, grey lines), and this saddled deviation is much smaller than that in molecules **A** and **B**. The molecules **C** and **D** are more loosely packed than molecules **A** and **B** because the overall thermal factors of molecules **C** and **D** are larger than those of molecules **A** and **B** (compare the thermal ellipsoids in Figure 6b and c). This means that Cl_4TBP–Zn can easily adopt both out-of-plane distortions depending on the surrounding environment. In all cases, the out-of-plane distortions are larger than those of the corresponding Cl_nTBCODP–Zn molecules (see Figure 3), which is easily rationalized by the steric effect of β,β-BCOD or β,β-benzene fusion towards the *meso* position. The distances between the γ-carbon atoms (2^1 and 2^4 positions) with no substituent at the *meso* position are in the range 5.5–5.7 Å in TBPs **3** and 6.1–6.3 Å in TBCODPs **2**, respectively. These distances are elongated as a result of chlorine substitution at the *meso* positions.

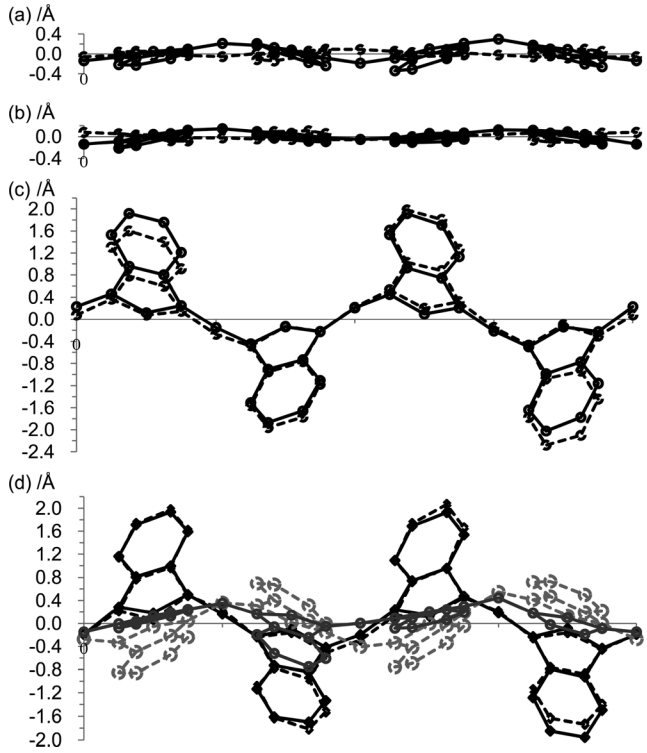

Figure 5. View of the skeletal deviations of the 40 ring atoms of TBPs from the porphyrin mean plane. (a) **3a**-Zn·3/2C_5H_5N from C_5H_5N/MeOH, two independent molecules; solid and broken lines; (b) **3a**-Zn·3/2C_5H_5N from C_5H_5N/*i*-C_3H_7OH: two independent molecules; solid and broken lines; (c) **3d**-Zn·3/2C_5H_5N·1/2MeOH: two independent molecules; solid and broken lines; (d) **3d**-Zn·5/4C_5H_5N·3/4*i*-C_3H_7OH: two pairs of independent stacked molecules; black solid (molecule **A**), black broken (molecule **B**), grey solid (molecule **C**), and grey broken lines (molecule **D**).

Next we made FET devices from the Cl_nTBP-H_2s **3a**-H_2 and **3d**-H_2 by the solution-based fabrication process. A chloroform solution of Cl_nTBCODPs **2** was spin-coated onto a heavily n-doped silicon wafer as substrate, and amorphous films of **3** were obtained. Then the films obtained were heated at 180 °C for 10 min to give thin films of Cl_nTBPs **3**. After the source and drain gold electrodes had been fabricated, the device performance of Cl_nTBPs **3** was measured. Only the device made from **3a**-H_2 showed FET characteristics: $\mu = 2.1 \times 10^{-4}$ $cm^2 V^{-1} s^{-1}$, $V_t = 16$ V, and $I_{on}/I_{off} = 10^2$. No FET performance was recorded with the device made from Cl_4TBP–Zn, which might be related to the flexible distorting nature of the porphyrin ring of Cl_4TBP–Zn because good OFET materials such as pentacene, TBP, and rubrene have rigid π systems irrespective of the flat or distorted nature of their π planes.[25]

Conclusions

We have succeeded in the preparation of *meso*-chlorinated benzoporphyrins (Cl_nTBPs) **3** by *meso*-chlorination of BCOD-fused porphyrin **1** with NCS followed by a thermal retro-Diels–Alder reaction. We also observed the unexpected *meso*-chlorination of the porphyrin with DDQ. We have clearly shown that the *meso* positions of quadruply BCOD-fused porphyrins (TBCODPs) are reactive and the BCOD moieties are robust towards electrophilic reactions. Moreover, the *meso* positions are less hindered than in TBPs. Therefore, this method, which involves the use of TBCODPs as precursors of TBPs, opens a new route to the preparation of variously *meso*-functionalized TBPs. The introduction of chlorine at the *meso* positions of TBP significantly changes the electronic and structural properties. The OFET device based on the solution process using ClTBCODP-H_2 (**2a**-H_2) showed moderate performance as a FET.

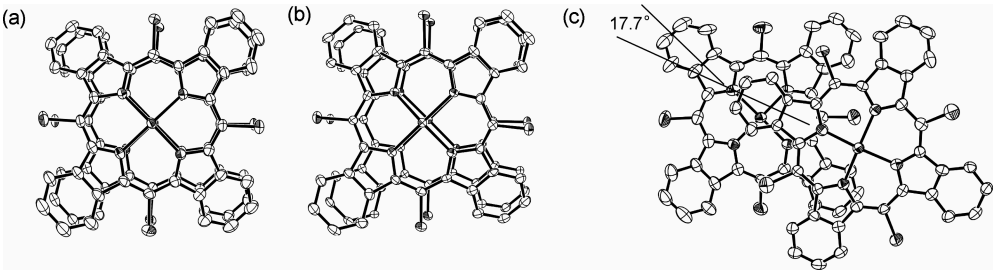

Figure 6. ORTEP diagrams (at the 50% probability level) viewed perpendicular to the stacked pairs: (a) in the $P\bar{1}$ crystal, (b) molecules **A** and **B** in $P2_1/c$, and (c) molecules **C** and **D** in $P2_1/c$. Solvent and hydrogen atoms have been omitted for clarity.

Experimental Section

General: Melting points were measured with a Yanaco MP-S_3 or M500-D melting-point apparatus. ^1H and ^{13}C NMR spectra were recorded with a JEOL JNM-AL 400, JNM-EX 400, or Varian VXR-500 spectrometer by using tetramethylsilane as the internal standard. UV spectra were recorded with a JASCO V-630 spectrophotometer. IR spectra were recorded with a Hitachi 270-30 or JASCO FT/IR-430 spectrometer by using KBr disks. FAB and DI-EI mass spectra were recorded with a JEOL JMS-700 instrument. MALDI-TOF mass spectra were recorded with a Voyager DE Pro (Applied Biosystems) or Autoflex II (Bruker Daltonics) instrument. Elemental analyses were performed with a Yanaco MT-5 elemental analyzer. All solvents and chemicals were of reagent-grade quality, obtained commercially, and used without further purification, except as noted. Dry dichloromethane and THF were purchased from Kanto Chemical Co. Toluene, hexane, triethylamine, pyridine, DBU, and chloroform were distilled from calcium hydride and then stored over appropriate molecular sieves. Solvents for chromatography were purified by distillation. For spectral measurements, spectral grades of toluene and chloroform were purchased from Nacalai Tesque Co. Thin-layer (TLC) and column chromatography were performed with Art. 5554 (Merck KGaA) and Silica Gel 60N (Kanto Chemical Co.), respectively. TBCODP-H_2 (**1**-H_2) was prepared according to a literature procedure.[11]

Typical Procedure for the Synthesis of *meso*-Chlorinated Porphyrins (Table 1, Entry 4): A mixture of *N*-chlorosuccinimide (56 mg, 0.44 mmol) and TBCODP-H_2 (**1**-H_2; 62 mg, 0.10 mmol) in chloroform (15 mL) was refluxed under Ar. After 72 h, the mixture was cooled and washed successively with an aqueous saturated $NaHCO_3$ solution, water (3×), and brine. The organic layer was dried with anhydrous Na_2SO_4 and concentrated. The residual solid was purified by column chromatography on silica gel (chloroform/hexane, 7:3) to give a maroon powder, which was then triturated with aqueous MeOH to give pure Cl_4TBCODP-H_2 (**2d**-H_2, 53.2 mg, 70%). The analytical samples were obtained by trituration or recrystallization from a mixed solvent of $CHCl_3/CH_2Cl_2$/EtOH/MeOH/H_2O.

5-Chloro-2^1,2^4,7^1,7^4,12^1,12^4,17^1,17^4-tetrahydro-2^1,2^4,7^1,7^4,12^1,12^4,17^1,17^4-tetraethano-21*H*,23*H*-tetrabenzo[*b*,*g*,*l*,*q*]porphine (ClTBCODP-H_2; 2a-H_2): Maroon powder (mixture of isomers); m.p. >200 °C (decomp.). ^1H NMR ($CDCl_3$, 500 MHz, 25 °C): δ = 10.31 (m, 2 H, 10-, 20-H), 10.22 (s, 1 H, 15-H), 7.13 (m, 8 H, olefin-H), 6.39 (m, 2 H, bridgehead-H), 5.74 (m, 6 H, bridgehead-H), 2.21 (m, 8 H, axial-CH_2), 1.94 (m, 8 H, equatorial-CH_2), –4.21 (br. s, 2 H, NH) ppm. ^{13}C NMR ($CDCl_3$, 100 MHz, 25 °C): δ = 27.19, 27.23, 27.25, 27.84, 36.18, 36.33, 36.38, 39.88, 96.94, 97.49, 136.01, 136.68, 137.50, 147.95, 148.92, 149.92, 151.43 (typical signals) ppm. MS (MALDI-TOF): *m*/*z* = 656 $[M]^+$. UV/Vis ($CHCl_3$): λ_{max} [log(ε/M^{-1}cm^{-1})] = 397 [5.16], 502 [4.23], 534 [3.64], 573 [3.79], 625 [3.02] nm. $C_{44}H_{37}ClN_4\cdot 1/2H_2O$ (666.27): calcd. C 79.32, H 5.75, N 8.41; found C 79.38, H 5.68, N 8.29.

5,10-Dichloro-2^1,2^4,7^1,7^4,12^1,12^4,17^1,17^4-tetrahydro-2^1,2^4,7^1,7^4,12^1,12^4,17^1,17^4-tetraethano-21*H*,23*H*-tetrabenzo[*b*,*g*,*l*,*q*]porphine (*adj*-Cl_2TBCODP-H_2; *adj*-2b-H_2): Maroon powder (mixture of isomers); m.p. >200 °C (decomp.). ^1H NMR ($CDCl_3$, 500 MHz, 25 °C): δ = 10.05 (s, 2 H), 7.07 (m, 8 H, olefin-H), 6.47 (m, 2 H, bridgehead-H), 6.30 (m, 2 H, bridgehead-H), 5.64 (m, 4 H, bridgehead-H), 2.18 (m, 8 H, axial-CH_2), 1.94 (m, 8 H, equatorial-CH_2), –3.98 (br. s, 2 H, NH) ppm. ^{13}C NMR ($CDCl_3$, 100 MHz, 25 °C): δ = 26.20, 27.02, 27.09, 27.09, 27.18, 27.71, 27.83, 29.70, 35.91, 36.07, 36.16, 39.39, 97.16, 135.82, 136.52, 136.64, 136.73, 137.36, 145.79, 147.33 (typical signals) ppm. MS (MALDI-TOF): *m*/*z* 690 $[M]^+$. UV/Vis ($CHCl_3$): λ_{max} [log(ε/M^{-1}cm^{-1})] = 412 [5.19], 511 [4.36], 587 [4.00], 639 [3.74] nm. $C_{44}H_{36}Cl_2N_4\cdot H_2O\cdot 1/2CHCl_3$ (751.40): calcd. C 69.47, H 5.04, N 7.28; found C 69.05, H 5.05, N 6.94.

5,15-Dichloro-2^1,2^4,7^1,7^4,12^1,12^4,17^1,17^4-tetrahydro-2^1,2^4,7^1,7^4,12^1,12^4,17^1,17^4-tetraethano-21*H*,23*H*-tetrabenzo[*b*,*g*,*l*,*q*]porphine (*opp*-Cl_2TBCODP-H_2; *opp*-2b-H_2): Maroon powder (mixture of isomers); m.p. >200 °C (decomp.). ^1H NMR ($CDCl_3$, 500 MHz, 25 °C): δ = 10.23 (s, 2 H, 10-, 20-H), 7.12 (m, 8 H, olefin-H), 6.31 (m, 4 H, bridgehead-H), 5.73 (m, 4 H, bridgehead-H), 2.00 (m, 8 H, axial-CH_2), 1.89 (m, 8 H, equatorial-CH_2), –3.54 (br. s, 2 H, NH) ppm. ^{13}C NMR ($CDCl_3$, 100 MHz, 25 °C): δ = 20.89, 27.17, 36.15, 39.55, 135.86, 137.37, 147.91, 152.18 (typical signals) ppm. MS (MALDI-TOF): *m*/*z* = 690 $[M]^+$. UV/Vis ($CHCl_3$): λ_{max} [log(ε/M^{-1}cm^{-1})] = 409 [5.17], 511 [4.34], 542 [4.02], 584 [3.99], 636 [3.69] nm. $C_{44}H_{36}Cl_2N_4\cdot H_2O$ (709.71): calcd. C 74.46, H 5.40, N 7.89; found C 74.34, H 5.28, N 7.60.

5,10,15-Trichloro-2^1,2^4,7^1,7^4,12^1,12^4,17^1,17^4-tetrahydro-2^1,2^4,7^1,7^4,12^1,12^4,17^1,17^4-tetraethano-21*H*,23*H*-tetrabenzo[*b*,*g*,*l*,*q*]porphine (Cl_3TBCODP-H_2; 2c-H_2): Purple powder (mixture of isomers); m.p. >200 °C (decomp.). ^1H NMR ($CDCl_3$, 500 MHz, 25 °C): δ = 9.89 (s, 1 H, 20-H), 7.07 (m, 8 H, olefin-H), 6.32 (m, 4 H, bridgehead-H), 6.20 (m, 2 H, bridgehead-H), 5.58 (m, 2 H, bridgehead-H), 2.17 (m, 8 H, axial-CH_2), 1.81 (m, 8 H, equatorial-CH_2), –3.38 (br. s, 2 H, NH) ppm. ^{13}C NMR ($CDCl_3$, 100 MHz, 25 °C): δ = 26.03, 26.12, 27.01, 27.22, 29.71, 35.97, 36.15, 39.55, 136.53, 137.19 (typical signals; other signals were not observed at 25 °C) ppm. MS (MALDI-TOF): *m*/*z* = 725 $[M]^+$. UV/Vis ($CHCl_3$): λ_{max} [log(ε/M^{-1}cm^{-1})] = 422 [5.55], 523 [4.61], 559 [4.09], 603 [4.11], 660 [3.86] nm. $C_{44}H_{35}Cl_3N_4\cdot 2H_2O\cdot CH_3OH$ (792.24): calcd. C 68.05, H 5.46, N 7.05; found C 67.81, H 5.20, N 7.33.

5,10,15,20-Tetrachloro-2^1,2^4,7^1,7^4,12^1,12^4,17^1,17^4-tetrahydro-2^1,2^4,7^1,7^4,12^1,12^4,17^1,17^4-tetraethano-21*H*,23*H*-tetrabenzo[*b*,*g*,*l*,*q*]-porphine (Cl_4TBCODP-H_2; 2d-H_2): Purple powder (mixture of isomers); m.p. >200 °C (decomp.). ^1H NMR ($CDCl_3$, 400 MHz, 25 °C): δ = 6.80 (m, 8 H, olefin-H), 6.08 (m, 8 H, bridgehead-H), 2.07 (m, 8 H, axial-CH_2), 1.82 (m, 8 H, equatorial-CH_2), –2.80 (br. s, 2 H, NH) ppm. ^{13}C NMR ($CDCl_3$, 100 MHz, 25 °C): δ = 25.91, 25.99, 26.04, 26.11, 29.71, 39.05, 114.78, 136.23, 136.30 (typical signals; other signals were not observed at 25 °C) ppm. UV/Vis ($CHCl_3$): λ_{max} [log(ε/M^{-1}cm^{-1})] = 434 [5.89], 537 [4.84], 577 [4.64], 621 [4.42], 683 [4.41] nm. MS (MALDI-TOF): *m*/*z* = 760 $[M]^+$. $C_{44}H_{34}Cl_4N_4\cdot 5/2CHCl_3$ (1059.04): calcd. C 51.03, H 3.36, N 5.12; found C 51.38, H 3.02, N 4.96.

Typical Procedure for the Synthesis of the *meso*-Chlorinated Porphyrin–Zinc Complexes 2-Zn: A solution of **2d**-H_2 (76 mg, 0.10 mmol) and $Zn(OAc)\cdot 2H_2O$ (0.10 mg, 0.54 mmol) in $CHCl_3$/MeOH (9:1) was stirred at room temp. for 1 h. The solution was washed with water (3×) and brine. The organic layer was dried with anhydrous Na_2SO_4 and concentrated. The residual solid was purified by short column chromatography on silica gel (chloroform) to give a maroon powder, which was then triturated with aqueous MeOH to give pure Cl_4TBCODP–Zn (**2d**-Zn; 75.9 mg, 93%).

(5-Chloro-2^1,2^4,7^1,7^4,12^1,12^4,17^1,17^4-tetrahydro-2^1,2^4,7^1,7^4,12^1,12^4,17^1,17^4-tetraethanotetrabenzo[*b*,*g*,*l*,*q*]porphyrinato)zinc(II) (ClTBCODP–Zn; 2a-Zn): Purple powder (mixture of isomers); m.p. >200 °C (decomp.). ^1H NMR ($CDCl_3$, 500 MHz, 25 °C): δ = 10.35 (s, 2 H, 10-, 15-H), 10.32 (s, 1 H, 20-H), 7.14 (m, 8 H, olefin-H), 6.47 (m, 2 H, bridgehead-H), 5.75 (m, 6 H, bridgehead-H), 2.23 (m, 8 H, axial-CH_2), 1.95 (m, 8 H, equatorial-CH_2) ppm. ^{13}C NMR ($CDCl_3$, 100 MHz, 25 °C): δ = 27.23, 27.35, 27.95, 36.21,

36.46, 40.57, 97.88, 98.37, 136.13, 136.18, 136.85, 141.34, 142.47, 143.32, 149.35, 149.41, 150.25, 150.33, 151.99, 152.03 (typical signals) ppm. MS (MALDI-TOF): m/z = 718 $[M]^+$. UV/Vis ($CHCl_3$): λ_{max} [log(ε/M^{-1}cm^{-1})] = 409 [5.44], 535 [4.24], 573 [3.84] nm. $C_{44}H_{35}Cl_4N_4Zn{\cdot}CH_3OH$ (751.69): calcd. C 71.81, H 5.22, N 7.44; found C 72.02, H 5.20, N 7.17.

(5,10-Dichloro-2^1,2^4,7^1,7^4,12^1,12^4,17^1,17^4-tetrahydro-2^1,2^4,7^1,7^4,12^1,12^4,17^1,17^4-tetraethanotetrabenzo[*b*,*g*,*l*,*q*]porphyrinato)zinc(II) (*adj*-Cl$_2$TBCODP–Zn; *adj*-2b-Zn): Purple powder (mixture of isomers); m.p. >200 °C (decomp.). ^{1}H NMR ($CDCl_3$, 500 MHz, 25 °C): δ = 10.15 (s, 2 H, 15-, 20-H), 7.11 (m, 8 H, olefin-H), 6.55 (m, 2 H, bridgehead-H), 6.38 (m, 2 H, bridgehead-H), 5.69 (m, 4 H, bridgehead-H), 2.35 (m, 8 H, axial-CH_2), 2.01 (m, 8 H, equatorial-CH_2) ppm. ^{13}C NMR ($CDCl_3$, 100 MHz, 25 °C): δ = 26.28, 27.12, 27.12, 27.22, 27.83, 27.95, 29.71, 36.13, 36.42, 39.95, 40.75, 98.01, 136.05, 136.75, 136.98, 137.63, 142.31, 143.55, 149.99, 150.65, 151.32, 152.32 (typical signals) ppm. MS (MALDI-TOF): m/z = 752 $[M]^+$. UV/Vis ($CHCl_3$): λ_{max} [log(ε/M^{-1}cm^{-1})] = 419 [5.24], 546 [4.03], 589 [3.56] nm. $C_{44}H_{34}Cl_2N_4Zn{\cdot}3/2CH_3OH$ (801.65): calcd. C 68.04, H 5.02, N 6.98; found C 68.22, H 5.00, N 6.51.

(5,15-Dichloro-2^1,2^4,7^1,7^4,12^1,12^4,17^1,17^4-tetrahydro-2^1,2^4,7^1,7^4,12^1,12^4,17^1,17^4-tetraethanotetrabenzo[*b*,*g*,*l*,*q*]porphyrinato)zinc(II) (*opp*-Cl$_2$TBCODP–Zn; *opp*-2b-Zn): Purple powder (mixture of isomers); m.p. >200 °C (decomp.). ^{1}H NMR ($CDCl_3$, 500 MHz, 25 °C): δ = 10.24 (s, 2 H, 10-, 20-H), 7.12 (m, 8 H, olefin-H), 6.43 (m, 4 H, bridgehead-H), 5.73 (m, 4 H, bridgehead-H), 2.03 (m, 8 H, axial-CH_2), 1.90 (m, 8 H, equatorial-CH_2) ppm. ^{13}C NMR ($CDCl_3$, 100 MHz, 25 °C): δ = 27.16, 27.27, 29.71, 36.14, 40.51, 98.76, 136.01, 137.68, 141.42, 142.31, 149.71, 152.49 (typical signals) ppm. MS (MALDI-TOF): m/z = 752 $[M]^+$. UV/Vis ($CHCl_3$): λ_{max} [log(ε/M^{-1}cm^{-1})] = 417 [5.25], 546 [4.00], 583 [3.42] nm. $C_{44}H_{34}Cl_2N_4Zn{\cdot}H_2O{\cdot}CH_3OH$ (804.15): calcd. C 67.13, H 5.01, N 6.96; found C 67.53, H 4.67, N 6.77.

(5,10,15-Trichloro-2^1,2^4,7^1,7^4,12^1,12^4,17^1,17^4-tetrahydro-2^1,2^4,7^1,7^4,12^1,12^4,17^1,17^4-tetraethanotetrabenzo[*b*,*g*,*l*,*q*]porphyrinato)zinc(II) (Cl$_3$TBCODP–Zn; 2c-Zn): Purple powder (mixture of isomers); m.p. >200 °C (decomp.). ^{1}H NMR ($CDCl_3$, 500 MHz, 25 °C): δ = 10.00 (s, 1 H, 20-H), 7.07 (m, 8 H, olefin-H), 6.43 (m, 4 H, bridgehead-H), 6.30 (m, 2 H, bridgehead-H), 5.63 (m, 2 H, bridgehead-H), 2.13 (m, 8 H, axial-CH_2), 1.92 (m, 8 H, equatorial-CH_2) ppm. ^{13}C NMR ($CDCl_3$, 100 MHz, 25 °C): δ = 25.61, 26.22, 26.31, 26.39, 27.13, 27.26, 27.26, 27.37, 29.71, 36.09, 36.20, 39.71, 39.79, 39.91, 39.96, 40.04, 40.45, 40.54, 40.61, 97.87, 114.17, 135.90, 135.95, 136.09, 136.13, 136.78, 136.81, 136.85, 137.47, 137.65, 140.59, 141.09, 141.45, 142.25, 142.52, 142.76, 149.82, 150.90, 152.03 (typical signals) ppm. MS (MALDI-TOF): m/z = 786 $[M]^+$. UV/Vis ($CHCl_3$): λ_{max} [log(ε/M^{-1}cm^{-1})] = 430 [5.54], 558 [4.48] nm. $C_{44}H_{33}Cl_3N_4Zn{\cdot}4CH_3OH$ (913.68): calcd. C 62.82, H 5.38, N 6.11; found C 62.74, H 5.14, N 6.26.

(5,10,15,20-Tetrachloro-2^1,2^4,7^1,7^4,12^1,12^4,17^1,17^4-tetrahydro-2^1,2^4,7^1,7^4,12^1,12^4,17^1,17^4-tetraethanotetrabenzo[*b*,*g*,*l*,*q*]porphyrinato)zinc(II) (Cl$_4$TBCODP–Zn; 2d-Zn): Purple powder (mixture of isomers); m.p. >200 °C (decomp.). ^{1}H NMR ($CDCl_3$, 400 MHz, 25 °C): δ = 6.85–7.15 (m, 8 H, olefin-H), 6.39 (m, 8 H, bridgehead-H), 1.73–2.50 (m, 16 H, CH_2) ppm. ^{13}C NMR ($CDCl_3$, 100 MHz, 25 °C): δ = 25.98, 29.71, 39.74, 39.81, 136.67, 151.11 (typical signals; other signals were not observed at 25 °C) ppm. UV/Vis ($CHCl_3$): λ_{max} [log(ε/M^{-1}cm^{-1})] = 442 [5.43], 576 [4.34], 621 [3.95] nm. MS (MALDI-TOF): m/z = 820 $[M]^+$. $C_{44}H_{32}Cl_4N_4Zn{\cdot}2H_2O$ (860.02): calcd. C 61.45, H 4.22, N 6.51; found C 61.51, H 4.26, N 6.50.

5-Chloro-21*H*,23*H*-tetrabenzo[*b*,*g*,*l*,*q*]porphine (ClTBP-H$_2$; 3a-H$_2$): Green powder; m.p. >200 °C. MS (MALDI-TOF): m/z = 545 $[M]^+$. UV/Vis (1% TFA/$CHCl_3$): λ_{max} (relative intensity) = 455 (100), 612 (4.2), 666 (25.2) nm. $C_{36}H_{21}ClN_4$ (545.05): calcd. C 79.33, H 3.88, N 10.28; found C 78.94, H 3.99, N 10.10.

5,10-Dichloro-21*H*,23*H*-tetrabenzo[*b*,*g*,*l*,*q*]porphine (*adj*-Cl$_2$TBP-H$_2$; *adj*-3b-H$_2$): Green powder; m.p. >200 °C. MS (MALDI-TOF): m/z = 578 $[M]^+$. UV/Vis (1% TFA/$CHCl_3$): λ_{max} (relative intensity) = 442 (43.4), 460 (100), 663 (8.8) nm. $C_{36}H_{20}Cl_2N_4$ (579.49): calcd. C 74.62, H 3.48, N 9.67; found C 75.03, H 3.33, N 9.44.

5,15-Dichloro-21*H*,23*H*-tetrabenzo[*b*,*g*,*l*,*q*]porphine (*opp*-Cl$_2$TBP-H$_2$; *opp*-3b-H$_2$): Green powder; m.p. >200 °C. MS (MALDI-TOF): m/z = 578 $[M]^+$. UV/Vis (1% TFA/$CHCl_3$): λ_{max} [log(ε/M^{-1}cm^{-1})] = 425 [4.67], 451 [5.49], 595 [4.10], 641 [4.71] nm. $C_{36}H_{20}Cl_2N_4$ (579.49): calcd. C 74.62, H 3.48, N 9.67; found C 74.64, H 3.67, N 9.50.

5,10,15-Trichloro-21*H*,23*H*-tetrabenzo[*b*,*g*,*l*,*q*]porphine (Cl$_3$TBP-H$_2$; 3c-H$_2$): Green powder; m.p. >200 °C. MS (MALDI-TOF): m/z = 612 $[M]^+$. UV/Vis (1% TFA/$CHCl_3$): λ_{max} (relative intensity) = 461 (77.0), 472 (100), 616 (4.5), 678 (6.5) nm. $C_{36}H_{19}Cl_3N_4$ (613.94): calcd. C 70.43, H 3.12, N 9.13; found C 70.00, H 2.97, N 9.43.

5,10,15,20-Tetrachloro-21*H*,23*H*-tetrabenzo[*b*,*g*,*l*,*q*]porphine (Cl$_4$TBP-H$_2$; 3d-H$_2$): Green powder; m.p. >200 °C. MS (MALDI-TOF): m/z = 646 $[M]^+$. UV/Vis (1% TFA/$CHCl_3$): λ_{max} (relative intensity) = 464 (12.6), 494 (100), 649 (4.4), 707 (5.4) nm. $C_{36}H_{18}Cl_4N_4$ (648.38): calcd. C 66.69, H 2.80, N 8.64; found C 66.81, H 2.46, N 8.77.

(5-Chlorotetrabenzo[*b*,*g*,*l*,*q*]porphyrinato)zinc(II) (ClTBP–Zn; 3a-Zn): Green powder; m.p. >200 °C. ^{1}H NMR (5% C_5D_5N/$CDCl_3$, 500 MHz, 25 °C): δ = 10.53 (s, 2 H, 10-, 20-H), 10.35 (s, 1 H, 15-H), 10.22 (m, 2 H, Ar-H), 9.54 (m, 2 H, Ar-H), 9.38 (m, 4 H, Ar-H), 8.17 (m, 8 H, Ar-H) ppm. MS (MALDI-TOF): m/z = 606 $[M]^+$. UV/Vis ($CHCl_3$): λ_{max} [log(ε/M^{-1}cm^{-1})] = 440.5 [5.50], 415 [4.56], 588 [4.02], 633 [4.86] nm. $C_{36}H_{19}ClN_4Zn{\cdot}H_2O$ (626.45): calcd. C 69.02, H 3.38, N 8.94; found C 68.88, H 3.49, N 8.85.

(5,10-Dichlorotetrabenzo[*b*,*g*,*l*,*q*]porphyrinato)zinc(II) (*adj*-Cl$_2$TBP–Zn; *adj*-3b-Zn): Green powder; m.p. >200 °C. ^{1}H NMR (5% C_5D_5N/$CDCl_3$, 500 MHz, 25 °C): δ = 10.40 (s, 2 H, 15-, 20-H), 10.35 (m, 2 H, Ar-H), 10.14 (m, 2 H, Ar-H), 9.48 (m, 2 H, Ar-H), 9.31 (m, 2 H, Ar-H), 8.15 (m, 8 H, Ar-H) ppm. MS (MALDI-TOF): m/z = 640 $[M]^+$. UV/Vis ($CHCl_3$): λ_{max} [log(ε/M^{-1}cm^{-1})] = 451 [5.49], 425 [4.67], 599 [4.10], 641 [4.71] nm. $C_{36}H_{18}Cl_2N_4Zn{\cdot}CH_3OH$ (673.92): calcd. C 65.84, H 3.29, N 8.30; found C 66.01, H 3.34, N 8.08.

(5,15-Dichlorotetrabenzo[*b*,*g*,*l*,*q*]porphyrinato)zinc(II) (*opp*-Cl$_2$TBP–Zn; *opp*-3b-Zn): Green powder; m.p. >200 °C. ^{1}H NMR (5% C_5D_5N/$CDCl_3$, 500 MHz, 25 °C): δ = 10.64 (s, 2 H, 10-, 20-H), 10.19 (m, 4 H, Ar-H), 9.53 (m, 4 H, Ar-H), 8.16 (m, 8 H, Ar-H) ppm. MS (MALDI-TOF): m/z = 640 $[M]^+$. UV/Vis ($CHCl_3$): λ_{max} [log(ε/M^{-1}cm^{-1})] = 449 [5.40], 422 [4.55], 596 [4.12], 640 [4.66], 729 [3.90] nm. $C_{36}H_{18}Cl_2N_4Zn{\cdot}H_2O$ (660.90): calcd. C 65.43, H 3.05, N 10.73; found C 65.58, H 3.04, N 10.78.

(5,10,15-Trichlorotetrabenzo[*b*,*g*,*l*,*q*]porphyrinato)zinc(II) (Cl$_3$TBP–Zn; 3c-Zn): Green powder; m.p. >200 °C. ^{1}H NMR (5% C_5D_5N/$CDCl_3$, 500 MHz, 25 °C): δ = 10.36 (s, 1 H, 20-H), 10.21 (m, 2 H, Ar-H), 10.17 (m, 2 H, Ar-H), 10.02 (m, 2 H, Ar-H), 9.40 (m, 2 H, Ar-H), 8.10 (m, 4 H, Ar-H), 8.03 (m, 4 H, Ar-H) ppm. UV/Vis ($CHCl_3$): λ_{max} [log(ε/M^{-1}cm^{-1})] = 464 [5.66], 610 [4.42], 653 [4.77] nm. MS (MALDI-TOF): m/z = 674 $[M]^+$. $C_{36}H_{17}Cl_3N_4Zn{\cdot}H_2O$

(695.34): calcd. C 62.18, H 2.75, N 8.06; found C 62.24, H 3.11, N 7.89.

(5,10,15,20-Tetrachlorotetrabenzo[*b*,*g*,*l*,*q*]porphyrinato)zinc(II) (Cl_4TBP–Zn; 3d-Zn): Green powder; m.p. >200 °C. ^{1}H NMR (5% C_5D_5N/$CDCl_3$, 400 MHz, 25 °C): δ = 10.11 (m, 8 H, Ar-H), 8.03 (m, 8 H, Ar-H) ppm. UV/Vis ($CHCl_3$): λ_{max} [log(ε/M^{-1}cm^{-1})] = 483 [5.52], 630 [4.35], 678 [4.60] nm. MS (MALDI-TOF): *m*/*z* = 708 $[M]^+$. $C_{36}H_{16}Cl_4N_4Zn{\cdot}CH_3OH$ (742.81): calcd. C 59.75, H 2.71, N 7.53; found C 59.79, H 3.16, N 7.52.

5-Chloro-2,3,7,8,12,13,17,18-tetraethyl-21*H*,23*H*-porphine (ClOEP-H_2; 4a-H_2): Red-brown powder; m.p. >200 °C. ^{1}H NMR ($CDCl_3$, 400 MHz, 25 °C): δ = 10.09 (s, 2 H, 10-, 20-H), 9.88 (s, 1 H, 15-H), 4.21 (q, *J* = 7.02 Hz, 2 H), 4.06 (m, 12 H, CH_2), 1.88 (m, 24 H, CH_3), –3.13 (br. s, 2 H, NH) ppm. ^{13}C NMR (1% TFA/$CDCl_3$, 100 MHz, 25 °C): δ = 16.46, 17.20, 17.30, 17.32, 19.67, 19.83, 19.92, 20.85, 98.55, 112.92, 141.37, 142.72, 142.91, 144.33 ppm. MS (MALDI-TOF): *m*/*z* = 569 $[M]^+$. UV/Vis ($CHCl_3$): λ_{max} [log(ε/M^{-1}cm^{-1})] = 408 [5.28], 507 [4.21], 541 [3.79], 579 [3.81], 629 [3.31] nm. $C_{36}H_{45}ClN_4{\cdot}CH_2Cl_2$ (654.17): calcd. C 67.93, H 7.24, N 8.56; found C 68.20, H 6.85, N 8.60.

5,15-Dichloro-2,3,7,8,12,13,17,18-tetraethyl-21*H*,23*H*-porphine (*opp*-Cl_2OEP-H_2; *opp*-4b-H_2): Purple powder; m.p. >200 °C. ^{1}H NMR ($CDCl_3$, 400 MHz, 25 °C): δ = 10.01 (s, 2 H, 10-, 20-H), 4.13 (m, 16 H, CH_2), 1.85 (m, 24 H, CH_3) 2.20 (br. s, 2 H, NH) ppm. ^{13}C NMR ($CDCl_3$, 100 MHz, 25 °C): δ = 16.90, 18.43, 19.75, 22.60, 97.45, 111.25, 140.61, 142.16, 144.08, 145.31 ppm. MS (MALDI-TOF): *m*/*z* = 603 $[M]^+$. UV/Vis ($CHCl_3$): λ_{max} [log(ε/M^{-1}cm^{-1})] = 415 [5.22], 515 [4.17], 550 [3.65], 588 [3.72], 642 [2.93] nm. $C_{36}H_{44}Cl_2N_4{\cdot}1/2CH_3OH$ (619.20): calcd. C 70.74, H 7.48, N 9.04; found C 71.10, H 7.13, N 9.40.

Supporting Information (see footnote on the first page of this article): Crystallographic summaries of Cl_nTBCODPs **2** and Cl_nTBPs **3**.[26]

[1] R. P. Linstead, E. G. Noble, *J. Chem. Soc.* **1937**, 933–936.
[2] S. Aramaki, Y. Sakai, N. Ono, *Appl. Phys. Lett.* **2004**, *84*, 2085–2087; Z. Bao, A. J. Lovinger, J. Dodabalapur, *Appl. Phys. Lett.* **1996**, *69*, 3066–3068; G. de Oteyza, E. Barrena, J. O. Osso, S. Sellner, H. Dosch, *J. Am. Chem. Soc.* **2006**, *128*, 15052–15053.
[3] T. D. Lash, *Energy Fuels* **1993**, *2*, 166–171; T. Fukuda, E. A. Makarova, E. A. Luk'yanets, N. Kobayashi, *Chem. Eur. J.* **2004**, *10*, 117–133; N. Kobayashi, S. Nakajima, H. Ogata, T. Fukuda, *Chem. Eur. J.* **2004**, *10*, 6294–6312.
[4] H. Tajalli, J. P. Jiang, J. T. Murray, N. R. Armstrong, A. Schmidt, M. Chandross, S. Mazumdar, N. Peyghambarian, *Appl. Phys. Lett.* **1995**, *67*, 1639–1641; J. S. Shirk, R. G. S. Pong, F. J. Bartoli, A. W. Snow, *Appl. Phys. Lett.* **1993**, *63*, 1880–1882; N. Ono, S. Ito, C. H. Wu, C. H. Chen, T. C. Wen, *Chem. Phys.* **2000**, *262*, 467–473.
[5] R. Bonnett, *Chem. Soc. Rev.* **1995**, *24*, 19–33.
[6] O. Senge in *The Porphyrin Handbook*, vol. 1 (Eds.: K. M. Kadish, K. M. Smith, R. Guilard), Academic Press, New York, **1999**, chapter 6, pp. 280–283.
[7] H. Anderson, *Chem. Commun.* **1999**, 2323–2330.
[8] a) R. Bonnett, G. F. Stephenson, *J. Org. Chem.* **1965**, *30*, 2791–2798; L.-C. Gong, D. Dolphin, *Tetrahedron Lett.* **1976**, *17*, 2197–2200; E. Watanabe, S. Nishimura, H. Ogoshi, Z. Yoshida, *Tetrahedron* **1975**, *31*, 1385–1390; b) Y. Naruta, F. Tani, K. Maruyama, *Tetrahedron Lett.* **1992**, *33*, 1069–1072.
[9] a) M. G. H. Vincente, A. C. Tome, A. Walter, J. A. S. Cavalerio, *Tetrahedron Lett.* **1997**, *38*, 3639–3642; M. G. H. Vincente, L. Jaquinod, R. G. Khoury, A. Y. Madrona, K. M. Smith, *Tetrahedron Lett.* **1999**, *40*, 8763–8766; b) S. Ito, H. Uno, T. Murashima, N. Ono, *Tetrahedron Lett.* **2001**, *42*, 45–47; T. Murashima, S. Tsujimoto, T. Yamada, T. Miyazawa, H. Uno, N. Ono, N. Sugimoto, *Tetrahedron Lett.* **2005**, *46*, 113–116.
[10] G. A. Molander (Ed.), "Catalyst Components for Coupling Reactions" in *Handbook of Reagents for Organic Synthesis*, Wiley, New York, **2008**.
[11] S. Ito, T. Murashima, H. Uno, N. Ono, *Chem. Commun.* **1998**, 1661–1662; S. Ito, N. Ochi, T. Murashima, H. Uno, N. Ono, *Heterocycles* **2000**, *52*, 399–411.
[12] H. Yamada, T. Okujima, N. Ono, *Chem. Commun.* **2008**, 2957–2974.
[13] M. Nencki, J. Zaleski, *Ber. Dtsch. Chem. Ges.* **1901**, *34*, 997–1010.
[14] H. Fischer, W. Neumann, *Justus Liebigs Ann. Chem.* **1932**, *494*, 225–245; H. Fischer, H. Roese, *Ber. Dtsch. Chem. Ges.* **1913**, *46*, 2460–2466.
[15] R. Bonnett, I. A. D. Gale, G. F. Stephenson, *J. Chem. Soc. C* **1966**, 1600–1604.
[16] L.-C. Gong, D. Dolphin, *Can. J. Chem.* **1985**, *63*, 406–411.
[17] L.-M. Jin, J.-J. Yin, L. Chen, C.-C. Guo, Q.-Y. Chen, *Synlett* **2005**, 2893–2898.
[18] The chloride ion from DDQ has been reported to attack the 2,2′-anhydro bond of 5,6-dihydropyrimidine nucleosides, see: P. V. P. Pragnacharyulu, E. Abushanab, *Tetrahedron Lett.* **1997**, *38*, 3683–3686.
[19] R. Bonnett, I. H. Campion-Smith, A. N. Kozyrev, A. F. Mironov, *J. Chem. Res. (S)* **1990**, 138–139; R. Bonnett, I. H. Campion-Smith, A. N. Kozyrev, A. F. Mironov, *J. Chem. Res. (M)* **1990**, 1001–1009.
[20] M. O. Senge, "Highly Substituted Porphyrins" in *The Porphyrin Handbook* (Eds.: K. M. Kadish, K. M. Smith, R. Guilard), Academic Press, San Diego, **1999**, vol. 1, chapter 6, pp. 239–347.
[21] H. Uno, Y. Shimizu, H. Uoyama, Y. Tanaka, T. Okujima, N. Ono, *Eur. J. Org. Chem.* **2008**, 87–98.
[22] S. Ito, H. Uno, T. Murashima, N. Ono, *Chem. Commun.* **1999**, 2275–2276.
[23] N. Ono, H. Hironaga, K. Ono, S. Kaneko, T. Murashima, T. Ueda, C. Tsukamura, T. Ogawa, *J. Chem. Soc. Perkin Trans. 1* **1996**, 417–423; T. D. Lash, P. Chandrasekar, *J. Am. Chem. Soc.* **1996**, *118*, 8767–8768; N. Ono, T. Yamamoto, N. Shimada, K. Kuroki, M. Wada, R. Utsunomiya, T. Yano, H. Uno, T. Murashima, *Heterocycles* **2003**, *61*, 447–453.
[24] *PLATON, A Multipurpose Crystallographic Tool*: A. L. Spek, *J. Appl. Crystallogr.* **2003**, *36*, 7–13.
[25] V. C. Sundar, J. Zaumseil, V. Podzorov, E. Menard, R. L. Willett, T. Someya, M. E. Gershenson, J. A. Rogers, *Science* **2004**, *303*, 1644–1647.
[26] X-ray data were processed by using CrystalClear Ver. 1.3.6. The processed data were treated with the CrystalStructure and WinGX programs. Structures were solved by SIR-97, expanded by DIRDIF, and then refined by SHELXL-97. The final structures were validated by the PLATON cif check. *CrystalStructure, Crystal structure analysis package*, Ver. 3.8.2, Rigaku (3-9-12 Akishima, Tokyo, Japan) and Rigaku/MSC (9009 New Trails Dr., The Woodlands, TX 77381 USA), **2000**–**2004**. WinGX 1.80.03: Suite for small-molecule single-crystal crystallography, University of Glasgow: L. J. Farrugia, *J. Appl. Crystallogr.* **1999**, *32*, 837–838. SIR-97: A package for crystal structure solution and refinement, Istituto di Gristallografia, Italy: A. Altomare, M. C. Burla, M. Camalli, G. Cascarano, C. Giacovazzo, A. Guagliardi, A. G. G. Moliterni, G. Polidori, R. Spagna, *J. Appl. Crystallogr.* **1999**, *32*, 115–119. G. M. Sheldrick, *SHELXL-97: Program for the refinement of crystal structures from diffraction data*, University of Göttingen, **1998**. "A short history of SHELX": G. M. Sheldrick, *Acta Crystallogr., Sect. A* **2008**, *64*, 112–122. P. T. Beurskens, G. Beurskens, R. de Gelder, S. Garcia-Granda, R. O. Gould, J. M. M. Smits, *DIRDIF2008*, Crystallography Laboratory, University of Nijmegen, The Netherlands, **2008**. CCDC-732084 (**2a**-$H_2{\cdot}CHCl_3$), -732086 (*opp*-**2b**-$H_2{\cdot}CHCl_3$), -732085 (*opp*-**2b**-

Zn·C_5H_5N), -732087 (**2d**-Zn·2MeOH), -732083 (**3a**-Zn·3/2C_5H_5N), -732082 (**3a**-Zn·3/2C_5H_5N), -732081 (**3d**-Zn·6C_5H_5N·1/2*i*-C_3H_7OH), -732080 (**3d**-Zn·5/4C_5H_5N·3/4MeOH) contain the supplementary crystallographic data for this paper. These data can be obtained free of charge from The Cambridge Crystallographic Data Centre via www.ccdc.cam.ac.uk/data_request/cif.

Received: June 1, 2009
Published Online: September 18, 2009

